The anti-reflection lens: quantitatively far-field imaging beyond the Rayleigh limit

***Lianlin Li*[1], *and Fang Li*[2]**

[1,]School of EECS, Peking University, Beijing, 100871, China
Lianlin.li@pku.edu.cn
[1,]Institute of Electronics, Chinese Academy of Sciences, Beijing, 100090, China
fli@mail.ie.ac.cn

Abstract

This study reports an novel approach to reconstruct quantitatively the electrical parameters of imaged specimen with sub-wavelength resolution. This super-resolution imaging methodology relies on the use of anti-reflection lens with the property of zero (strictly, approximately zero) backward propagation. We demonstrate theoretically and numerically that the anti-reflection lenses can encode the subtle information of imaged specimen into far field, and thus support the quantitative reconstruction of probed objects in the sub-wavelength resolution from far-field measurements merely by solving a well-conditioned linear inverse problem. The proposed approach is not only confined to weakly- but also suitable for generally- scattering cases. The operational principle of constructing the anti-reflection lens that is achievable with current experimental technique is provided as well. This new approach will be a breakthrough in the spatio-temporal control of field (or light) with the potential of being applied in nanolithography, detection, sensing or sub-wavelength imaging in the near future.

1. Introduction

Over more than a century, numerous attempts have been made to bypass the Rayleigh limit. Among them the most famous one is based on so-called near-field scanning optical microscopy (NSOM), whereby the sub-wavelength imaging could be achieved by detecting both propagating and evanescent waves through a scanning tip close proximity to the undergoing sub-wavelength specimen [1]. In the last few years several intriguing ideas have also been proposed to relief more or less the strong requirement of near-field scanning for the sub-wavelength imaging. Two representative instruments are *superlens* [2]and *hyperlens*[3], both of which are made of artificial materials exhibiting some abnormal electromagnetic behaviors. However, subsequent studies demonstrated that the superlens implementation is severely curtailed due to material losses or the characteristic patterning of the negative index systems. Additionally, the hyperlens consists of an extremely thick ring (or partial ring), and its size determines directly the imaging resolution. Recently, Lemoult et al improve the method consisting lens of a well-suitable spatial-temporal dispersive medium, which encodes the spatial finer features of imaged objects in an ultra-wideband temporal signal [4].

This study reports an approach that is capable of quantitatively reconstructing the electrical parameters of imaged specimen with sub-wavelength resolution. This methodology relies on the anti-reflection lens with the property of zero backward propagation [5]. The anti-reflection lens consists of materials in the sub-wavelength scale, and is placed in the vicinity of probed objects. Consequently, the finer features of the equivalent current induced in probed objects, both radiating currents and non-radiating currents, can be encoded or modulated by the anti-reflections lens, and transferred to the far field. As a consequence, employing a series of anti-reflection lenses with different sub-wavelength structures will substantially increase the number of independent measurements, thus overcoming the ill-posedness of undergoing inverse problem can being accomplished. Once the equivalent currents embedded in the probed objects are accurately reconstructed in a sub-wavelength resolution, the electrical parameters of the probed objects can be easily quantitatively calculated by performing straightforward algebraic implementations

978-1-4673-5225-3/14/$31.00 ©2014 IEEE

certainly with the sub-wavelength resolution.

2. Theoretical Derivation

For clarity the principle of proposed methodology here is restricted into the two-dimensional (2D) scalar case. Referring to Fig.1, the imaged object, which is illuminated by a monochromatic TM-polarized line source located at $(0, y_s)$, is situated on the left side of an anti-reflection lens. The measurements are acquired within the interval of [-L,L]along the line at a large distance $z_r \gg \lambda$. Additionally, the region of interest (ROI) where probed objects are embedded is denoted by D_1, and the area occupied by the anti-reflection lens byD_2.

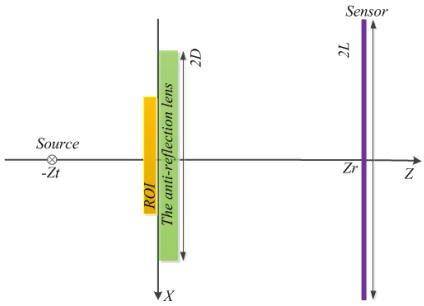

Fig.1 The geometrical configuration adopted to study the anti-reflection based super-resolution imaging

The z-polarized electrical fields inside D_1 and D_2 are governed by following coupled integral equations in compact form [6]:

$$\boldsymbol{E}_{t,1} = \boldsymbol{E}_{in,1} + k_0^2 \boldsymbol{G}_{1,2} \boldsymbol{E}_{t,2} \boldsymbol{\chi}_{lens} + k_0^2 \boldsymbol{G}_{1,1} \boldsymbol{E}_{t,1} \boldsymbol{\chi}_{obj} \tag{1a}$$

$$\boldsymbol{E}_{t,2} = \boldsymbol{E}_{in,2} + k_0^2 \boldsymbol{G}_{2,1} \boldsymbol{E}_{t,1} \boldsymbol{\chi}_{obj} + k_0^2 \boldsymbol{G}_{2,2} \boldsymbol{E}_{t,2} \boldsymbol{\chi}_{lens} \tag{1b}$$

where the subscripts of '1' and '2' highlight, respectively, the associated quantities related to the region D1 and D2. $\boldsymbol{G}_{i,j}$(i,j=1,2)denotes the matrix with entries of $G_0(\boldsymbol{r}.\boldsymbol{r}')$where $\boldsymbol{r} \in D_i$, and $\boldsymbol{r}' \in D_j$. $\boldsymbol{\chi}_{obj/lens}$represents the contrast of the probed objects (or the anti-reflection lens medium) with respect to background medium. Owing to zero-backward propagation of wavefields inside the anti-reflection lens, the coupled term in the Eq.(1a) falls off, that is：

$$\boldsymbol{T}_{12} = k_0^2 \boldsymbol{G}_{1,2} \boldsymbol{E}_{t,2} \boldsymbol{\chi}_{lens} = \boldsymbol{0} \tag{2}$$

Eq.(2) reveals that the electrical field inside D_1 induced by the equivalent current inside the anti-reflection lens $\boldsymbol{E}_{t,2}\boldsymbol{\chi}_{lens}$ can be ignored. Now the scattered field in the far field region reads as

$$E_{sca} = k_0^2 \boldsymbol{G}_{sca,} \boldsymbol{E}_{t,2} \boldsymbol{\chi}_{lens} = k_0^2 \boldsymbol{G}_{sca,} \boldsymbol{G}_{12} diag(\boldsymbol{\chi}_{lens}) \left(I - k_0^2 \boldsymbol{G}_{22} diag(\boldsymbol{\chi}_{lens})\right)^{-1} \boldsymbol{E}_{in,2}^{eq} \tag{3}$$

where $\mathbf{E}_{in,2}^{eq} = \mathbf{E}_{in,2} + k_0^2 \mathbf{G}_{2,1} diag(\chi_{obj}) \mathbf{E}_{t,1}$. Note that there is a spatial mixing between $\boldsymbol{E}_{in,2}^{eq}and\boldsymbol{\chi}_{lens}$, is operating in the Eq. (3). Such operation allows for encoding finer details of $\boldsymbol{E}_{in,2}^{eq}$ into far-field observations provided that$\boldsymbol{\chi}_{lens}$varies in the sub-wavelength scale. However, the dimension of scattering field$\boldsymbol{E}_{sca}$is remarkably lower than that of probed object for a fixed $\boldsymbol{\chi}_{lens}$, which cause that Eq. (3) is highly of ill-posedness. To resolve this problem, we put forward to employ multiple anti-reflection lenses as that proposed above to increase the number of independent measurements. As a consequence, the unique solution of $\boldsymbol{E}_{in,2}^{eq}$ can be readily obtained by solving the resulting well-conditioned linear equations. Once $\boldsymbol{E}_{in,2}^{eq}$ being obtained, the solution to $diag(\boldsymbol{\chi}_{obj})\boldsymbol{E}_{t,1}$ in sub-wavelength resolution can be exactly derived by solving Eq. (5).

Concerning the construction of the anti-reflection lens, Eq.(2) leads to

$$\boldsymbol{G}_{12} diag(\boldsymbol{\chi}_{lens}) \left(I - \boldsymbol{G}_{22} diag(\boldsymbol{\chi}_{lens})\right)^{-1} = \boldsymbol{0} \tag{4}$$

It is well accepted that$\boldsymbol{G}_{12}$is highly ill-posed and its null space can be spanned by its P right singular vectors corresponding to zero (or approximately zero) singular values. Eq.(4) shows that a great amount of solutions

toχ_{lens}can be derived , which means numerous anti-reflection lens can be readily devised.

3. Numerical Results

Here several numerical experiments are provided to demonstrate the performance of proposed super-resolution imaging methodology. The setup for our simulations is shown in Fig.1. For mimicking 2D scenario, both the anti-reflection lens and probed objects are assumed to be infinitely extended along *y*-direction, the imaged objects are confined into the region ROI, a thin rectangle of 10λx0.1λ in the *O-xz* plane, meanwhile the anti-reflection lens is assumed to be of a 20λx0.4λ rectangle, moreover the ideal TM-polarized line source is adopted in which the working wavelength λ is assigned to be 1mm. To build the anti-reflection lens for breaking the Rayleigh limit, a cluster of scatters is arranged on a sub-wavelength scale according that discussed above. In this simulation, the anti-reflection lens is composed of 10λ-length dielectric columns with0.1λx0.1λ square section, such 200 lenses are generated and random five of them are depicted in figure 2, The Fig. 2(a) shows the real parts of the contrast functions of 3 anti-reflection lenses, while Fig.2(b) is for the imaginary parts. Fig. 2 shows that the anti-reflection lens can be fabricated by using normal low-loss materials. Additionally, the input data for imaging simulation procedure are generated by performing a commonly used full-wave solver to Maxwell's equations, namely, the method of moment (MoM).

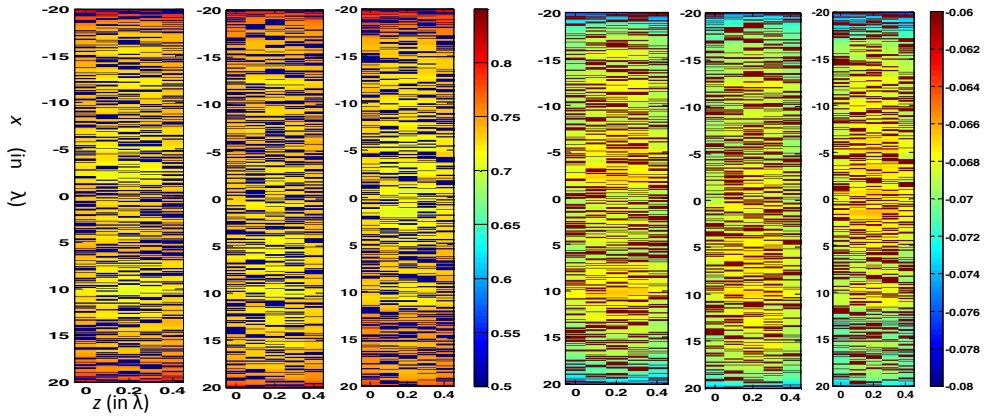

Fig.2 Three anti-reflection lenses used for super-resolution imaging, where the left are for real parts of the contrast functions, and the right for imaginary parts.

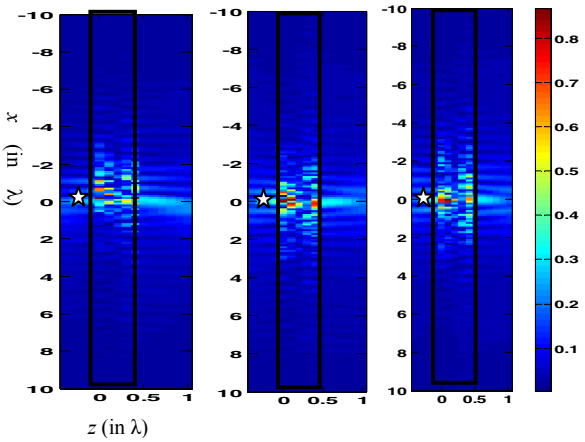

Fig.3 Results of zero backward propagation simulation. The scattered fields (the total electrical field minus incident component) corresponding to the case of five lenses (in the Fig. 2), the pentagrams and the black.el the sources and the

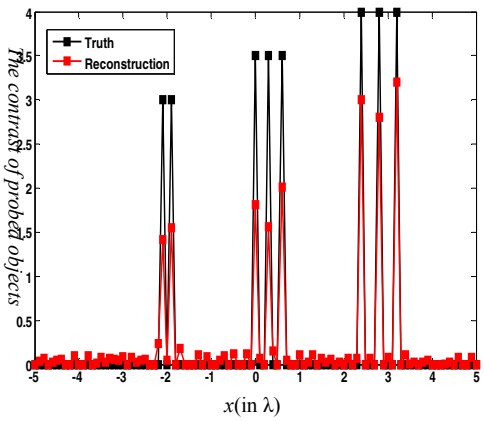

Fig. 4 Results of Quantitatively far-field imaging with sub-wavelength resolution simulation. The object consists of multiple dielectric bars with varying refraction displayed by black-filled squares 0.1λx 0.1λ. The imaging results displayed

Zero backward propagation simulation: To look insight into these lenses' property of zero backward propagation, they are illuminated by the TM-polarized line source placed at the location of z_t=-0.03λ and x_t=0. The amplitudes of scattered fields (the total electrical field minus incident component) corresponding to the case of five lenses in Fig. 2 are reported

in Fig. 3 (where the pentagrams and the black squares label the sources and the anti-reflection lenses, respectively). It shows that a majority of incident energy resides in and passes through the anti-reflection lens, while only a small portion is reflected. Meanwhile, the distinct radiation patterns on a sub-wavelength scale are supported by using different anti-reflection lenses, and this spatial information reaches the far-field, giving rise to extra degrees of freedom for measurements。 From another view, the results also indicate that the anti-reflection lens make it feasible to deposit field (or optical) energy on a deep sub-wavelength scale from the far-field dynamically, which promises the potential applications in nanolithography or sensing.

Quantitatively far-field imaging with sub-wavelength resolution simulation: In the simulation, the probed objects are placed 0.0362mm left of the anti-reflection lens. The object consists of multiple dielectric bars with varying refraction, as displayed in the Figure 4, where a square is of cross-section 0.1λx 0.1λ. To show advantage of the spatial degrees of freedom offered by our designed lens, the simulation repeats the operation for 200 anti-reflection lenses, where SNRs are set at 35dB. Although non-exact reconstruction of ground truth due to non-ideal zero-backward propagation of the anti-reflection lenses, the image results shown in Fig. 4 clearly demonstrate that proposed anti-reflection lens can be applied to the sub-wavelength imaging from far-field measurements. In spite of the simplicity of these objects in the simulation, the first results provided here prove the innovative principle of this work: the sub-wavelength information of an object can be registered in the far-field region by spatial mixing of sub-wavelength structures through the anti-reflection lens.

4. Conclusion

In this study, we report an approach that enables to quantitatively reconstruct the electrical parameters of imaged specimen with sub-wavelength resolution. This methodology relies on the anti-reflection lens with the property of zero (strictly, approximately zero) backward propagation of both propagating and evanescent waves emerging from imaged objects. We theoretically and numerically demonstrate that the use of a series of the anti-reflection lenses allows us to quantitatively reconstruct the probed objects in a sub-wavelength resolution from far-field measurements by merely solving a well-conditioned linear inverse problem. We have performed a numerical proof of the concept of imaging below the diffraction limit from the far-field with a realistic medium. This proposed approach is at the frontiers but achievable with current experimental techniques. Additionally, all the performances of the proposed approach are not on the assumption of weakly scatter. It means that this new approach is not confined to weakly- but also suitable for generally- scattering cases. It is a significant breakthrough for the technique of field (or light) spatio-temporal control. It is expected that the proposed methodology will be applied in nanolithography, detection, sensing or sub-wavelength imaging in the near future.

5. References

[1] http://en.wikipedia.org/wiki/Near-field_scanning_optical_microscope

[2]P J. B. Pendry, Negative refraction makes a perfect lens, Phys. Rev. Lett., 85, 3966-3969, 2000

[3]Z. Jacob, L. V. Alekseyev and E. Narimanov, Optical hyperlens: far-field imaging beyond the diffraction limit, Optics Express, 14, 8247, 2006

[4] F. Lemoult, M. Fink and G. Lerosey, A polychromatic approach to far-field superlensing at visible wavelengths, Nature communications, 1885, 2012

[5] H. K. Raut, V. A. Ganesh, A. S. Nair and S. Ramakrishna, Anti-reflective coatings: A critical, in-depth review, Energy& Environmental Sciences, 4, 3779, 2011

[6]W. C. Chew, Waves and fields in inhomogeneous media, Piscataway, IJ: IEEE Press, 1996